A01-28158

AIAA-2001-1902

An Integrated Optimization for Conceptual Designs of Airbreathing Launch TSTO Vehicle

T. Tsuchiya, T. Mori and M. Maita
National Aerospace Laboratory of Japan
Tokyo, JAPAN

AIAA/NAL-NASDA-ISAS 10th International Space Planes and Hypersonic Systems and Technologies Conference
April 24-27, 2001 Kyoto JAPAN

AIAA-2001-1902

AN INTEGRATED OPTIMIZATION FOR CONCEPTUAL DESIGNS OF AIRBREATHING LAUNCH TSTO VEHICLE

Takeshi Tsuchiya*, Takashige Mori† and Masataka Maita†
National Aerospace Laboratory of Japan
Tokyo, JAPAN

Abstract

This paper presents the application of an optimization method to conceptual designs of fully reusable TSTO (Two-Stage-To-Orbit) spaceplanes. TSTO spaceplane is under consideration for the future space transportation vehicle Japan aims to develop and realize in the near future. Technical fields for vehicle designs in this paper are aerodynamic analysis, engine analysis, weight analysis, and trajectory analysis, which are integrated and optimized simultaneously by an optimization method proposed herein. A payload weight is defined as an index of the feasibility of spaceplanes, and the best shape and trajectories maximizing the payload weight are indicated. The results show the effectiveness of the proposed numerical methods and necessity of the further weight reduction to realize future space transportation vehicles.

Introduction

In the 21st century, many people expect further space activities. It partly depends on whether or not we can early realize low-cost fully reusable space transportation system to and from the earth.

Based upon the long-term space policy envisioned by the Space Activities Commission of Japan in 1996, the Science and Technology Agency established the Committee on Future Space Transportation System in April 1999. The Committee defined the new direction for Japan's future space transportation system for the 21st century. In June 2000, the Committee issued the report to propose incremental research and development program toward the final goal of SSTO (Single-Stage-To-Orbit) spaceplanes with the interim TSTO (Two-Stage-To-Orbit) spaceplane development[1]. Therefore, Japan has aimed to realize fully reusable TSTO system in a few decades.

TSTO vehicle considered in the report and this present paper is composed of a hypersonic booster plane and a reusable winged orbiter, as shown in Fig. 1. The booster is powered by airbreathing engines, ATREX engines[2], which have been developed in the Institute of Space and Astronautical Science (ISAS) of Japan. The orbiter has reusable LOX/LH_2 rocket engines. The booster carrying the orbiter on the body takes off horizontally at a lunch site, and accelerates with the ATREX engines. After performance limit of the ATREX engines, about Mach 6, the orbiter is separated. The booster flies back to the launch site after the separation. The orbiter continues its ascent to a circular orbit about the earth with the rocket engines. After the mission on the orbit, the orbiter reenters the atmosphere and returns to the launch site. It is assumed that they are unmanned vehicles, and orbiter's payload capability is 8 ton to LEO.

By the way, we have studied the integrated optimization for vehicle sizing and flight trajectories of SSTO spaceplanes[3]. Based on these results, the purpose of the present work is to apply these optimization methods into the multidisciplinary design optimization problem for

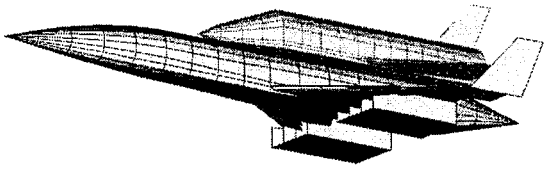

Fig. 1 TSTO spaceplane model

* Researcher, Space Transportation Project Center
† Senior Researcher, AIAA Member

the TSTO spaceplanes and to indicate the best vehicle shapes and their flight trajectories. In this study, payload capability to LEO is regarded as a feasibility index. The optimization problem finding the vehicle shape and the trajectory to maximize the payload weight of the orbiter is solved.

Analyzed Models

Firstly, the variables and models analyzed in the optimization problem are defined in this section. Figure 2 outlines the disciplines and the data flows among in this paper. The variables in need of our decision are classified into three types: the variables representing geometric shapes of the vehicles, flight performance, and flight trajectories. If a set of values are given to the variables, the disciplines are analyzed along the fig. 2 sequentially. The "analyze" herein means that the disciplines do not only calculate the variable values passed to other disciplines, but also compute function values C_E and C_I of the equality and inequality constraint conditions which the variables have to satisfy. It is necessary to find the variables satisfying these conditions.

The following summarizes the analyzed models and constraint conditions in each discipline.

Vehicle Configuration Design

Figures 1 and 3 show exteriors of TSTO vehicles in this study. The booster images a supersonic transport vehicle, and the orbiter shape refers to Space Shuttle Orbiter and HOPE-X[4] of Japan. ATERX engines of the booster are composed of six units and suspended on the lower surface of the wing, and one rocket engine is installed in the aft body of the orbiter. For lateral stability, the orbiter has a vertical tail plane, while the booster substitutes tipfins for vertical tail planes, because the orbiter lies on the upper surface of the body and the vertical planes are considered to have little effect. Areas of the tipfins and the vertical tail plane, and a body flap on the orbiter are specified by tail volume values required by HOPE-X[4] for their stability. They also have the same shape as those of HOPE-X.

In the vehicle configuration design, design variables concerning the body shape are shown in

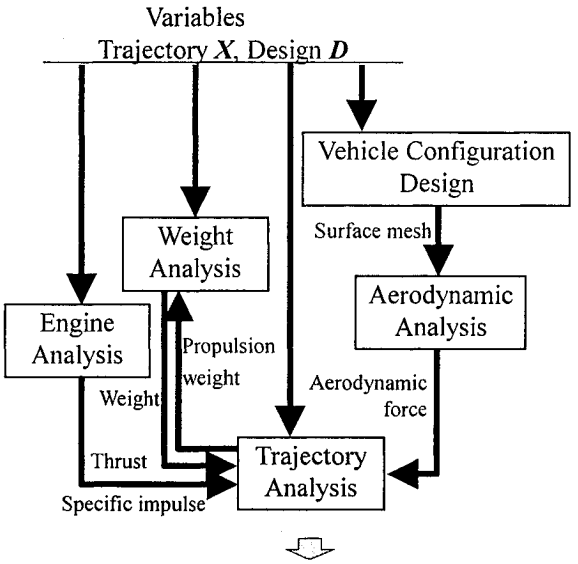

Fig. 2 Analyzed models

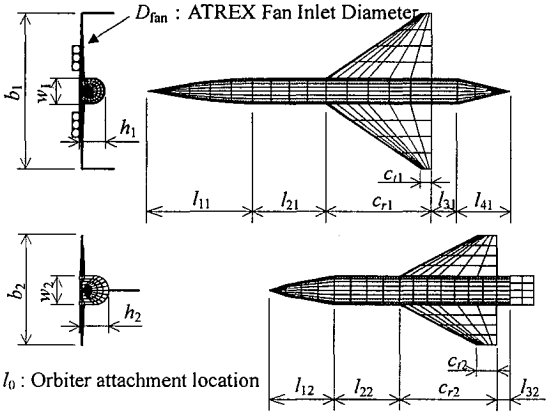

Fig. 3 Design variables for vehicle shapes

Fig. 3. The other variables are flight performance of the two vehicles; thrust limit of the booster, rocket thrust of the orbiter, load factor limit of each vehicle, and dynamic pressure limit of each vehicle. One aim in this process is to make surface meshes used in the following aerodynamic analysis. The optimum meshes are formed automatically and fast, as illustrated in Fig. 3.

Besides, there are some inequality constraint conditions which the variables have to satisfy. First, the variables concerning the body shape should hold reasonable values. These values are more than zero, and nose length and body fitness ratio are restricted within the effective range of the

aerodynamic analysis method. Similar constraints are applied to the variables regarding the flight performance. The load factor limits should be more than 2.5, and the dynamic pressure limits should be less than 50 kPa. In addition to these, tank volume of liquid hydrogen consumed by the ATREX engines restricts the minimum body size of the booster. The body size of the orbiter is also constrained by the liquid oxygen and hydrogen tanks and the payload bay volume (80 m^3).

Aerodynamic Analysis

The estimation of the aerodynamic vehicle properties has to consider the different flowfield regimes encountered during atmospheric flight covering the range from subsonic to hypersonic speed for two vehicles and the booster carrying the orbiter. For this purpose, simple methods are used. In the subsonic flight of the booster and the orbiter, a panel method[5] is employed. From supersonic to hypersonic speed Prandtl-Meyer expansion flow theory and tangent cone/wedge method are used along a panelized vehicle surface model. These methods are simpler than the latest sophistical computation methods but useful, because aerodynamic characteristics are analyzed over and over in the optimization method proposed in this paper. In spite of the problems of propulsion integration, control surface efficiencies, etc., which require more sophistical methods, these methods are applied widely for aerodynamic preliminary analysis[6].

However, these simple methods have a limit of application to various shapes of the airplanes. This study has to analyze the form that one vehicle lies on top of the other vehicle, which is beyond the limit. Thus, for the booster attached to the orbiter, the lift force is supposed to be equal to that of the booster, and the drag force is supposed to be the total drag of the booster and the parasite drag of the orbiter. It should be noted that aerodynamic interference between two vehicles makes an estimation error.

In this analysis, seven cases of Mach numbers and Reynolds numbers are selected, where the aerodynamic analysis competes the lift coefficient, drag coefficient and moment coefficient at several angles of attack. These coefficient values are approximated with polynomial expressions in each case, and the values between the cases are estimated with linear interpolation. It follows that the aerodynamic analysis requiring much computation time is implemented only after the body shapes are changed. The stored coefficient values of the polynomial can drastically shorten the computation time of the aerodynamic analysis iterated in the trajectory analysis.

Besides, longitudinal static stability of three forms is evaluated in subsonic and hypersonic regions, and aft limit of the center of gravity is calculated. Fore limit, which should be decided to achieve trim performance and maneuverability, is supposed to be 10 % forward location of the body length from the aft limit.

Engine Analysis

The ATREX engines of the booster can operate in less than about Mach 6 cruise. The engine performance is furnished by ISAS. Standard thrust force and specific impulse values are provided in response to Mach number and altitude. Fan inlet diameter is one of the design variables, and thrust force is proportional to the square of its value. Besides, the engines are installed on the bottom of the wings, and air compression by the fore body is not considered in this study.

The rocket thrust of the orbiter is one of the design variables and its specific impulse is fixed to be 450 sec independent of altitude and velocity.

Weight Analysis

The component weight in two vehicles is obtained with HASA model[7] from the body shape, flight performance, and the propellant weight provided by the trajectory analysis described below. The engine weight is, however, given in our own ways, because they cannot refer to the HASA model.

Below is the procedure of the weight analysis. First, the takeoff weight of the booster carrying the orbiter is supposed to be equal to gross weight of the booster, and the component weight of the booster is calculated with HASA program. Second, the difference of the summation of the component weight and the gross weight is the payload weight of the booster, which is equivalent to the gross

weight of the orbiter. Third, HASA is also employed to calculate the component weight of the orbiter, and the payload weight can be computed.

The components and subsystems are arranged to compute the center of gravity in the bodies which has full or empty propellant. There are some constraint conditions that the center of gravity in cases of full/empty propellant is within the limits given by the aerodynamic analysis.

Trajectory Analysis

The three-degree-freedom trajectory analysis of spaceplane is implemented. State variables are altitude h, longitude θ, latitude ϕ, velocity V, flight path angle γ, heading angle ψ, and mass m. Control variables are angle of attack α, and bank angle σ.

$$\dot{h} = V\sin\gamma \tag{1a}$$

$$\dot{\theta} = \frac{V\cos\gamma\cos\psi}{r\cos\phi} \tag{1b}$$

$$\dot{\phi} = \frac{V\cos\gamma\sin\psi}{r} \tag{1c}$$

$$\dot{V} = \frac{(T_{ATR}+T_{ROC})\cos\alpha - D}{m} - g\sin\gamma \tag{1d}$$

$$\dot{\gamma} = \frac{(T_{ATR}+T_{ROC})\sin\alpha + L}{mV}\cos\sigma - \left(\frac{g}{V}-\frac{V}{r}\right)\cos\gamma \tag{1e}$$

$$\dot{\psi} = \frac{(T_{ATR}+T_{ROC})\sin\alpha + L}{mV}\frac{\sin\sigma}{\cos\gamma} - \frac{V\cos\gamma\tan\phi\cos\psi}{r} \tag{1f}$$

$$\dot{m} = -\left(\frac{T_{ATR}}{I_{SP\,ATR}} + \frac{T_{ROC}}{I_{SP\,ROC}}\right)\frac{1}{g_0} \tag{1g}$$

where g and g_0 is the gravity acceleration at the altitude h and at the ground level, respectively, and r is distance from the Earth center.

Lift and Drag force L and D are defined by:

$$L = \frac{1}{2}\rho V^2 S_{ref} C_L \tag{2a}$$

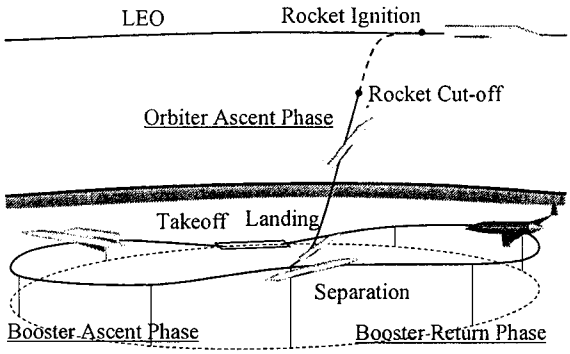

Fig. 4 Flight profile

$$D = \frac{1}{2}\rho V^2 S_{ref} C_D \tag{2b}$$

where the reference area S_{ref} is provided by the vehicle configuration design, the aerodynamic coefficients C_L and C_D are computed in the aerodynamic analysis, and U.S. Standard Atmosphere is employed for air density ρ. T_{ATR} and T_{ROC} are the thrust force of the ATREX engines and the rocket engines, respectively, and I_{SPATR} and I_{SPROC} present specific impulse of these engines. They are given by the engine analysis.

In this study, the flight before the orbiter reaches the orbit is divided into three phases, as shown in Fig 4. For the orbiter's return flight, especially, only the constraint conditions on its landing capability are considered, because they are the strongest conditions in the return flight.

Booster Ascent Phase — This phase presents the flight from the takeoff of the booster at the launch site to the separation of the booster and the orbiter. All ATREX engines operate at full throttle, while the rocket is not fired ($T_{ROC} = 0$). As characteristics of the ascent trajectory in this study, the vehicle does not fly on a vertical plane without the bank, but takes a turn. The reason is described bellow.

There are constraint conditions at the takeoff:

$$h = 0 \tag{3a}$$
$$\theta = 0 \tag{3b}$$
$$\phi = 0 \tag{3c}$$
$$V \le 100\ [\text{m/sec}] \tag{3d}$$
$$\gamma = 0 \tag{3e}$$
$$m = W_{takeoff} \tag{3f}$$
$$\sigma = 0 \tag{3g}$$

Takeoff weight W_{takeoff} is specified in the weight analysis. During the flight, path constraints are defined as:

$$h \geq 0 \tag{4a}$$

$$\frac{1}{2}\rho V^2 \leq q_{\max} \tag{4b}$$

$$\alpha \leq 20\,[\text{deg}] \tag{4c}$$

$$T_{\text{ATR}} \leq T_{\max} \tag{4d}$$

$$\frac{L\cos\alpha + D\sin\alpha}{mg} \leq n_{LF\max} \tag{4e}$$

where $q_{\max}$, $T_{\max}$, and $n_{LF\max}$ are maximum limit values of dynamic pressure, thrust force and load factor of the booster, respectively, which are the design variables. In addition, there are terminal conditions at the separation concerning pitch angle and bank angle:

$$\gamma + \alpha \geq 0 \tag{5a}$$

$$\sigma = 0 \tag{5b}$$

These expressions mean that the vehicles are separated with pitch angle more than zero and without the bank.

Orbiter Ascent Phase — This phase presents the flight that the released orbiter ascends to LEO. The orbiter accelerates and climbs above an altitude of 120 km with the rocket thrust force T_{ROC} which is specified as a design variable, and the engines stop firing. At the time, the orbiter is on the elliptical orbit whose apogee altitude is 300 km, and put into the circular orbit at the apogee point.

T_{ATR} in Eqs. (1a)-(1g) is fixed to be zero, and the aerodynamic coefficients C_L and C_D are those of the orbiter. The connection between the former phase and this phase makes some constraint conditions at the initial time of the present phase with regarding to the state variables, while the initial angle of attack is free. Obviously, the best bank angle is zero degrees during the flight. In addition, the same conditions as Eqs. (4a)-(4e) are constrained, though the maximum limit values are replaced by those of the orbiter. Terminal conditions at the rocket engine cut-off are expressed as

$$h \geq 120\,[\text{km}] \tag{6a}$$

$$\gamma \geq 0 \tag{6b}$$

and an equality condition that the apogee altitude computed from the terminal states should be 300 km.

Booster Return Phase — In this phase, the booster continues to fly from the separation and lands at the launch site finally.

A salient characteristics of the booster's flight path in this study is that the booster flies at full throttle in the ascent flight and returns to the launch site by gliding without the thrust in the return phase. Reference 1 reports the ascent flight on a vertical plane and the circuitous flying to reach the launch site by moderate closing the thrust. For this flight style, comparing with propellant consumption in the ascent phase, propellant requirement in the return phase is non-negligible. Moreover, in spite of the failure of the ATREX engines, safely to fly back to the launch site, the no powered vehicle are required to have the ability to return even from the separation point which is the farthest from the launch site. Besides, it has been reported that the trajectory optimization problems to minimize propellant weight or to maximize payload weight gives optimal solutions including bang-bang controls of thrust[8]. Therefore, the ATREX engines are ignited in maximum power in the booster ascent phase, and the throttle of the engines is shut in the booster return phase. To attain this performance, the booster circles not apart form the launch site, and the bank angle is controlled between zero and 90 degrees in the booster ascent phase and the booster return phase.

In this phase, T_{ATR} and T_{ROC} in Eqs. (1a)-(1g) are fixed to be zero, and the aerodynamic coefficients C_L and C_D of the booster are used. The motion equation of Eq. (1g) concerning mass can be removed, because the mass is constant. The connection between the booster ascent phase and this phase makes some constraints with regarding to the state and control variables at the initial time. The same conditions as Eqs. (4a)-(4e) are constrained. Terminal conditions at the landing are expressed as

$$h = 0 \tag{7a}$$

$$\theta = 0 \tag{7b}$$

$$\phi = 0 \quad (7c)$$

$$V \leq 100 \text{ [m/sec]} \quad (7d)$$

$$\gamma = 0 \quad (7e)$$

$$\sigma = 0 \quad (7f)$$

Optimization Problem

Performance Index

From the previous analyzed models, it is the lowest demand that the feasible variables satisfying all the constraint conditions are found. In these variables, to choose the best variables, the optimization problem is defined. In this paper, considering launch performance to LEO, the payload weight of the orbiter is defined as an maximized objective function presenting the feasibility of TSTO spaceplanes. The payload weight is obtained in the weight analysis.

Optimization Method

As the optimization method for the defined problem concerning the body design, flight performance and flight trajectory, block diagonal Hessian (BDH) method[9] is adopted. BDH method belongs to direct collocation methods for trajectory optimization problems, which transform these problems into nonlinear programming problems. By BDH method, the time domain is divided into some elements, and values of the state variables and the control variables are associated at each node connecting the elements. It follows from this that the motion equations represented as differential equations are also discretized into difference ones, and the nonlinear programming problems are defined. It is reported that this method has better convergence characteristics than the other direct collocation methods.

A weak point in BDH method is that the number of optimized variables is huge, and computation cost is expensive. In this problem, for example, there are nine state and control variables, and, as a consequence, the defined nonlinear programming problem has the variables in the amount of more than one thousand, which requires computers to bear large load.

Therefore, improved BDH method is thought up: all the state variables are not discretized, but some state values at the node are obtained by the numerical integration of the motion equations. The state variables θ, ϕ and ψ regarding horizontal position and lateral motion hardly influences the other variables h, V, γ, and m. In addition to this, the constraints concerning the variables θ, ϕ and ψ are only the conditions that the terminal coordinates in the booster return phase are equal to the origin, that is, the launch site. These implicitly lead us to the improved BDH method: the disretized state variables are only four variables, viz. altitude h, velocity V, flight path angle γ, and mass m, which have strong interrelation in the motion equations and the constraint conditions, and, in the analysis of the constraint conditions, the values of the other three state variables, longitude θ, latitude ϕ and heading angle ψ, are calculated by the numerical integration of these three motion equations.

Numerical Results

Optimal Design

An optimal shape and weight are shown in Fig. 5 and Table 1, where takeoff weight is fixed to 300 Mg. According to the optimal solution, the gross weight of the booster is 193.40 Mg, and that of the orbiter is 106.60 Mg, including only 0.88 Mg for a payload weight. To realize the TSTO system, the component weight reduction is necessary to increase the payload weight up to the practical weight, which is regarded as about 8 Mg in LEO.

Table 1 Optimal component weight

components	booster	orbiter
wing [Mg]	18.24	1.79
fuselage [Mg]	18.47	5.27
stabilizer [Mg]	—	0.53
TPS [Mg]	4.71	4.42
gear [Mg]	7.24	2.26
tank [Mg]	12.95	3.87
ATREX [Mg]	70.22	—
rocket [Mg]	—	2.17
LH_2 [Mg]	57.40	11.88
LOX [Mg]	—	71.28
payload [Mg]	—	0.88
misc. [Mg]	4.17	2.26
gross weight [Mg]	193.40	106.60

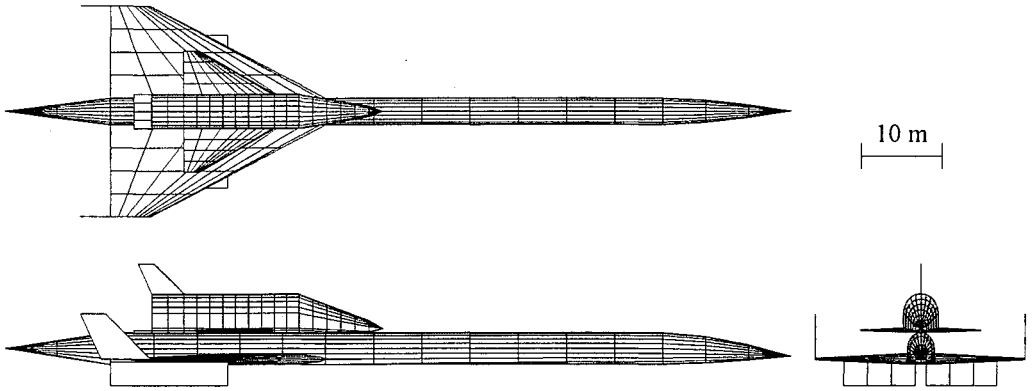

Fig. 5 Optimal shape

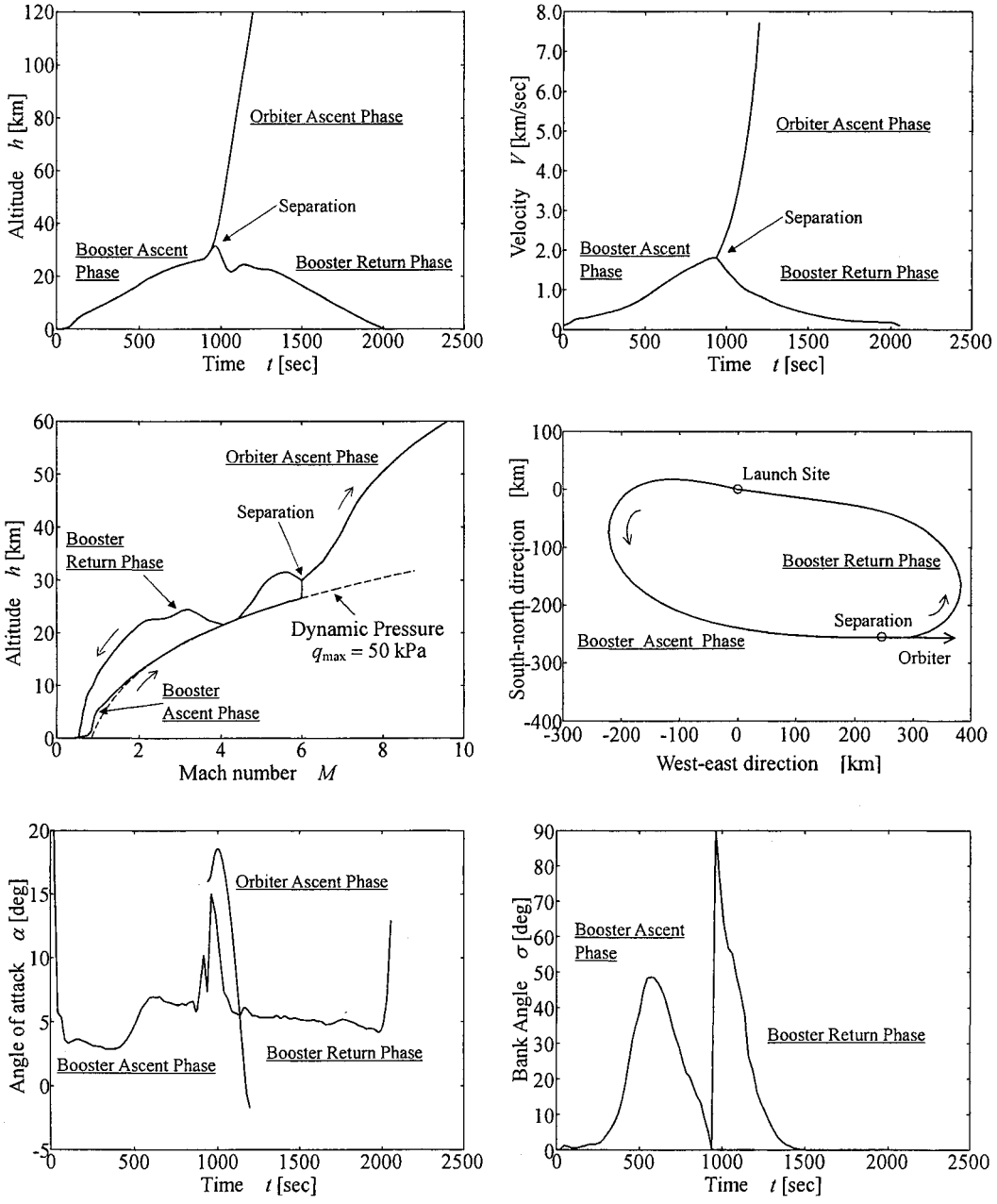

Fig. 6 Optimal trajectory

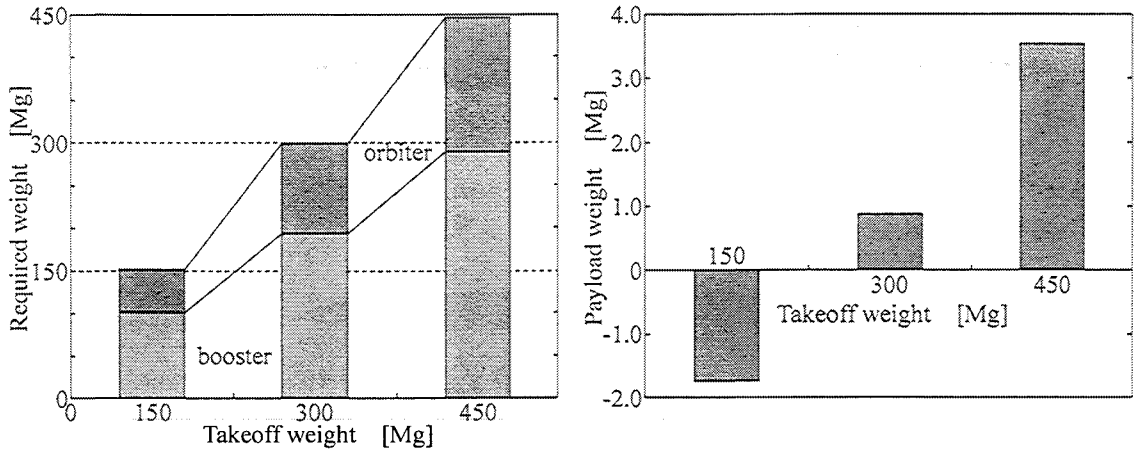

Fig. 7 Required weight and payload weight for takeoff weight

The optimal shape in Fig. 5 indicates that the booster has a very slender body with total length 99.3 m, width 3.3 m, and height 4.0 m to reduce the parasite drag. Large ATREX engines are, however, required to overcome the drag force. The engine weight amounts to 70.22 Mg, more than a half of the booster dry weight, and it is an open question whether the wing can support such large and heavy engines. Aerodynamic influence of the engine pods has not been considered. Moreover, the wing area of the booster is minimum limit to take off the vehicle with the angle of attack maximum.

The orbiter has a rocket engine with thrust force 1.40 MN for the gross weight of 106.60 Mg at the separation. The orbiter needs little force from its wing in the orbiter ascent phase, and the wing size is designed to satisfy the landing condition. Attachment location of the booster to the orbiter is given only by the requirement of the center of gravity, and aerodynamic interference between the two vehicles has not been considered.

Optimal Trajectory

Figure 6 shows the obtained optimal trajectory. After taking off with the angle of attack maximum and the bank angle zero degrees, the vehicle accelerates and rises slowly. When reaching dynamic pressure limit of 50 kPa, it flies along this limit. In addition to longitudinal control, it takes a turn with the bank control as indicated in Fig. 6. Just before attaining to Mach 6 that is operating limit of ATREX engines, the vehicle is pulled up and the altitude is gained to help the orbiter climb.

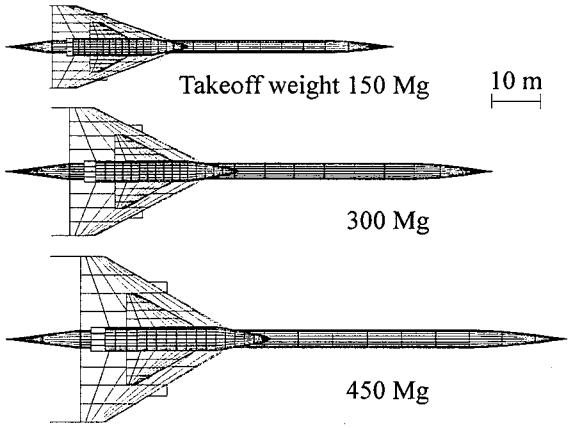

Fig. 8 Vehicle size for takeoff weight

At the separation, it reaches the altitude of 30 km, while it changes the heading angle of 196 deg to reach the launch site with no power. The dynamic pressure is 30 kPa at the separation, and it is not so high pressure that the orbiter cannot be released even in the vehicle configuration of this study. Immediately after the separation, the orbiter ignites the rocket engine, climbs up to the altitude of 120 km and reaches the elliptical orbit whose apogee altitude is 300 km. It should be noted that thrust vector of the rocket engine corresponds to the angle of attack.

While the orbiter continues to accelerate, the booster makes its bank angle maximum limit of 90 deg, and turns toward the launch site. In the second half of the return phase, the angle of attack is around the value which makes lift drag ratio maximum to extend flight range, and the booster can fly back to the site successfully.

Takeoff Weight and Payload Weight

Finally, the takeoff weight which has been fixed to 300 Mg is changed. Figures 7-8 show required weight, the payload weight and vehicle sizes for the takeoff weight. The required weight means total weight of the components except the payload, and the takeoff weight minus the required weight equals the payload weight. The payload weight in the takeoff weight of 150 Mg is negative, which means the orbiter cannot reach the LEO even without the payload. It is general that the weight estimation for future space transportation vehicles results in negative payload weight. Figure 7 indicates that the payload weight slightly increases with the takeoff weight. The increase of the takeoff weight cannot improve the feasibility of the TSTO spaceplanes in this study, and the weight reduction is the essential key issue to realize future space transportation systems.

Conclusions

The integrated optimization technique is applied into the conceptual designs of TSTO spaceplanes. First, analyzing tools are provided: surface mesh generator, simple aerodynamic analysis method, weight estimation method, and so on. Second, these analyzing models are integrated functionally and incorporated into an optimization method. A payload weight is defined as an objective function in the problem. The vehicle configurations and trajectories are found to maximize the payload weight. The solutions show the boosters of hypersonic vehicles which is slender body and have the huge ATREX engines. Future study should reconfirm weight and thrust force of the ATREX. In this study, the payload capability to LEO does not attain to 8 ton. Therefore, weight reduction of the components is required. In addition, through this study, it was confirmed that the proposed integrated optimization method was effective.

References

[1] Committee on Future Space Transportation System, "Committee on Future Space Transportation System—Final Report,", Science and Technology Agency , Jun. 2000 (in Japanese).

[2] Sato, T., Tanatsugu, N. and Naruo, Y. "Development Study on ATREX Engine," *Acta Astronautica*, Vol. 47, No. 11, 2000, pp. 799-808.

[3] Tsuchiya, T.: "An Integrated Optimization for Conceptual Designs of Spaceplane," *22nd International Congress of Aeronautical Sciences Proceedings*, Harrogate, 2000, Paper Number 7.4.1.

[4] NAL/NASDA HOPE joint research team, "Aerodynamic Data Book — HOPE-X FY09," NASDA-TMR-000001, 2000 (in Japanese).

[5] Morino, L., Chen, L., and Suciu, E., "Steady and Oscillatory Subsonic and Supersonic Aerodynamics around Complex Configurations," *AIAA Journal*, Vol. 13, No. 3, 1975, pp.368-374.

[6] Divan, P., "Aerodynamic Preliminary Analysis System 2. Part 2: User's Manuals," NASA-CR-165628, 1981.

[7] Harloff, G. J. and Berkowitz, B. M.: "HASA – Hypersonic Aerospace Sizing Analysis for Preliminary Design of Aerospace Vehicles," NASA CR-182226, 1988.

[8] Bryson, A. E., Jr. and Ho, Y. C.: "Applied Optimal Control," *Blaisdell Publishing Company*, MA, 1969.

[9] Tsuchiya, T. and Suzuki, S. "Spaceplane Trajectory Optimization with Vehicle Size Analysis," *14th IFAC Symposium on Automatic Control in Aerospace*, Seoul, 1998, pp. 444-449.